

pubs.acs.org/JACS Article

# Through-Space Electrochemiluminescence Reveals Bubble Forces at Remote Phase Boundaries

Brady R. Layman and Jeffrey E. Dick\*



Cite This: J. Am. Chem. Soc. 2024, 146, 707–713



**Read Online** 

**ACCESS** 

Metrics & More

Article Recommendations

Supporting Information

**ABSTRACT:** Several groups have reported on the curious chemistry and reaction acceleration in confined volumes. These complex multiphase systems most closely resemble natural processes, and new measurement tools are necessary to probe chemistry in such environments. Generally, electrochemiluminescence (ECL) reports on processes immediately near (within a few micrometers) the electrode surface. Here, we introduce through-space ECL, reporting on dynamics of processes far away (100s of  $\mu$ m) from the electrode surface. We achieved this by collecting reflected ECL light. During the heterogeneous oxidation of  $C_2O_4^{2^-}$  in an aqueous phase adjacent to a 1,2-dichlorethane droplet,  $CO_2$  accumulates in the 1,2-dichloroethane droplet. Upon buildup, we demonstrate that a  $CO_2$  bubble forms in the nonaqueous phase and is surprisingly trapped at the water|1,2-dichloroethane interface and continues to grow. The co-oxidation of tris(bipyridine)ruthenium(II) in the aqueous phase lights up the electrode surface and reflects off the edges of the bubble, revealing the bubble growth over time even when the bubble is fractions of a millimeter from the surface. We extend our results to quantifying bubble forces at the water—oil interface at remote distances from the electrode surface.



#### **■ INTRODUCTION**

Unique physicochemical properties and unexpected geometries are present in the multiphase environment, causing reactions to proceed in previously unexpected ways. 1,2 These multiphase environments exhibit interfaces like the liquidlliquid interface that have become of great interest to a broad community in science. An example of this broad interest in multiphase environments is Zwicker and colleagues' work to model mitosis in early protocells<sup>3</sup> and P granules behaving as liquids.<sup>4</sup> Additionally, new physiochemical phenomena are still being discovered. For instance, our group recently showed that when neighboring droplets fuse, microcompartments form. Such environments also have been implicated in the curious chemistry and reaction acceleration. Zare and co-workers have shown the ease of reducing carbon dioxide, nitrogen, and the generation of strong reducing agents in microdroplets.<sup>8,9</sup> Cooks and co-workers have also shown the immense reaction acceleration microdroplets can provide along with creating an environment for abiotic synthesis of peptide isomers. 10 Our group has also shown using stochastic nanoelectrochemistry that enzymatic rates can be enhanced by orders of magnitude in such environments. 11 This truth of nature regarding curious chemistry at phase boundaries necessitates new measurement science tools to understand the most fundamental tenets of chemistry in small multiphase places.

Electrochemiluminescence (ECL) is a surface-confined, light emission process in which a redox reaction gives rise to the emission of photons without the need for incident light for excitation. <sup>12</sup> The principle is as follows: If a luminophore is oxidized and a radical species donates an electron energetically enough, the electron has a probability of reaching an excited state in the luminophore. The excited state can then relax, generating a photon. ECL is used in a variety of applications from biology, <sup>13</sup> sensing devices, <sup>14</sup> and phase boundary determination. <sup>15,16</sup>

Since ECL is a surface-confined (a few micrometers) process, it is uniquely well-suited to examine multiple interfaces at one time. ECL is surface-confined because of the lifetimes of the electrogenerated excited-state species and radicals and can be used to map the liquidliquid and liquidl solid interfaces in multiphase systems. As an example, previous work from our group has shown that one can selectively emit photons from one phase in an emulsion. 16,18

Combining this electrochemical technique with an optical microscope allows us to selectively image light coming from specific phases to gain correlated electrochemical and optical information across interfaces. <sup>19</sup> However, the surface-confined nature of the ECL is a great limitation. One can imagine the benefits of using ECL to image processes rather far away from

Received: September 25, 2023 Revised: November 22, 2023 Accepted: November 27, 2023

Published: December 29, 2023





the electrode surface. Here, we develop a new method to use ECL through space while also answering important questions regarding multiphase microenvironments. As a model system, we drive the simultaneous oxidation of tris(bipyridine)ruthenium(II) in the presence of oxalate<sup>20</sup> on an electrode on which droplets of 1,2-dichloroethane are adsorbed. The oxidation of oxalate creates carbon dioxide (CO<sub>2</sub>). Because CO<sub>2</sub> is much more soluble in 1,2-dichloroethane than in water, carbon capture occurs in the nonaqueous phase. 21-24 The CO2, captured within the nonaqueous phase, nucleates and forms a bubble, which eventually detaches from the electrode and is surprisingly trapped at the waterloil interface, 100s of µm from the surface of the electrode. The reflected light reveals the bubble size and the violent moment when the bubble departs the nonaqueous phase. These results lay a foundation to use ECL in three dimensions and to learn important physicochemical properties of multiphase systems. Figure 1A shows a schematic representation of the experimental setup. A transparent indium tin oxide (ITO) electrode is used as the working electrode such that fresh emulsions can be imaged (Figure 1B). The previously established ECL mechanism for a tris(bipyridine)ruthenium-(II) ([Ru(bpy)<sub>3</sub>]<sup>2+</sup>) and sodium oxalate coreactant is shown below in Figure 1B. 20 In this reaction, [Ru(bpy)<sub>3</sub>]<sup>2+</sup> is oxidized to [Ru(bpy)<sub>3</sub>]<sup>3+</sup>. Simultaneously, the oxalate anion coreactant  $([C_2O_4]^{2-})$  is oxidized to  $[C_2O_4]^{\bullet-}$ . This radical anion then decomposes to one molecule of carbon dioxide and its radical anion ( $[CO_2]^{\bullet-}$ ), which behaves as a strong reducing agent. The  $[CO_2]^{\bullet-}$  reacts with  $[Ru(bpy)_3]^{3+}$  to form an excited state  $[Ru(bp)]_3^{2+*}$  and a molecule of carbon dioxide. The [Ru(bpy)<sub>3</sub>]<sup>2+\*</sup> radiatively relaxes and emits a photon.

#### ■ RESULTS AND DISCUSSION

The applied voltage to the system is +1.5 V, and an example of the resultant chronoamperometry is given in Figure S1. Previous work has shown that this applied voltage results in the greatest ECL intensity. 19 During the bubble growth phase, a spot of photons starts in the focal plane, as shown in Figure 2, and gradually becomes an out-of-focus ring as the bubble grows larger. This signal is what we term "through-space ECL" since it has an intermediate reflection step between the emission of photons and detection in the microscope system. An oil-in-water emulsion represents an ensemble of oil microdroplets in a continuous aqueous phase, all showing multiple orders of magnitude more solubility for CO<sub>2</sub> compared with the continuous water phase. To make this emulsion, 300 µL of the DCE phase was loaded into 5 mL of the aqueous phase and ultrasonicated (see the Materials and Methods section for complete description). Thus, the relatively large volume of DCE present in droplets at the electrode surface can act as a pump and reservoir for this CO<sub>2</sub> produced by the ECL reaction in the continuous aqueous phase. The nonaqueous droplets are effectively acting as small volumes for carbon capture.

In Figure 2, image 1 (495.95 s) is imaged before the appearance of a large  $CO_2$  bubble at the water|1,2-dichloroethane interface. Panel 2 shows the arrival of the  $CO_2$  bubble at the apex of the interface (496.95 s). Through the rest of the experiment, the growth of the bubble can be viewed along with the coalescence of different DCE droplets. A fluorescence image is taken at 523.87 s to show the difference between the smaller DCE droplets that are bright yellow (no  $CO_2$  bubble present) and the larger DCE droplet that is mostly taken up by

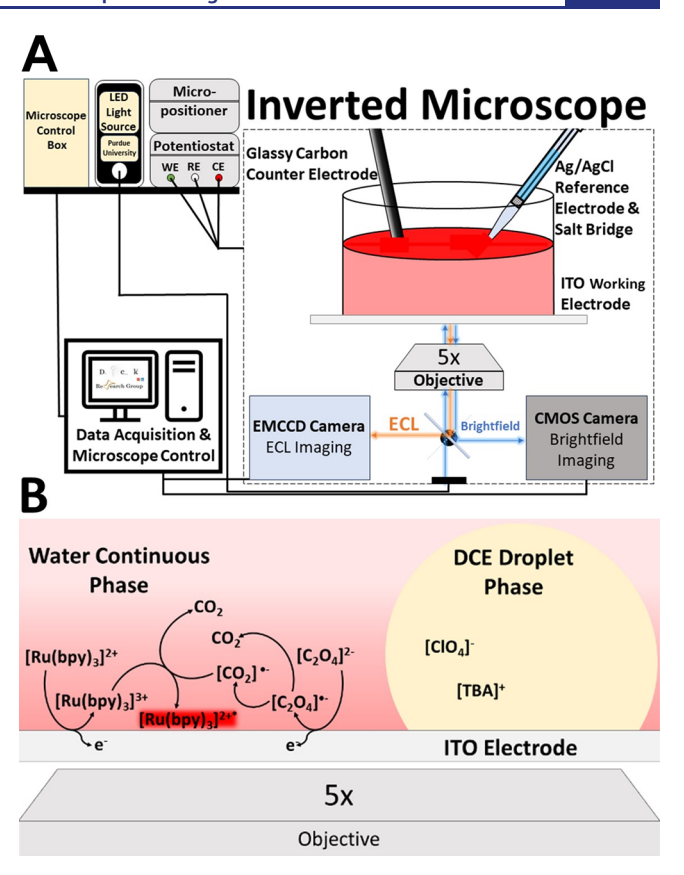


Figure 1. (A) Top schematic showing the coupled optoelectrochemical experimental setup. A computer controls the microscope and potentiostat. A glassy carbon rod is used as a counter electrode, Ag/ AgCl with a salt bridge composes the reference electrode, and an optical transparent ITO electrode is the working electrode. An EMCCD camera images the ECL microscopy, and a CMOS camera images the bright-field microscopy. The path of the bright-field (blue) and ECL signal (orange) is also shown from their origin and detector, with a dichroic mirror being able to direct the light path to a specific detector. (B) Bottom schematic showing the mechanism of the oxidative oxalate coreactant ECL pathway. <sup>20</sup> The cation luminophore  $([Ru(bpy)_3]^{2+})$  and oxalate anion coreactant  $([C_2O_4]^{2-})$  are oxidized. The newly formed radical anion ( $[C_2O_4]^{\bullet-}$ ) decomposes to carbon dioxide and its radical anion ( $[CO_2]^{\bullet-}$ ). This radical anion acts as a strong reducing agent with the previously oxidized luminophore cation ( $[Ru(bpy)_3]^{3+}$ ). This reaction produces an excited-state luminophore ([Ru(bpy)<sub>3</sub>]<sup>2+\*</sup>), which undergoes radiative relaxation to emit a photon along with a molecule of carbon dioxide.

the  $\mathrm{CO}_2$  bubble. The use of both techniques (ECL and fluorescence) can be a powerful mapping tool to understand complex chemistry in multiphase environments. The result that the bubble is somehow trapped at the waterl1.2-dichloroethane interface is surprising but can be explained by relative surface tensions in multiphase systems and bubble buoyancy (vide infra).

To further investigate this "through-space ECL" signal, specifically at the beginning of the nucleation (such as in panel 2 of Figure 2), a 15  $\mu$ L droplet of DCE was placed on the surface of an ITO electrode by hand with a pipet. The purpose and goal of this experiment (Figure 3) were to eliminate events such as droplet coalescence, which could potentially interfere with the observation of the CO<sub>2</sub> bubble.

The ECL reaction was initiated within a single pipet droplet submerged in water on the surface of an ITO electrode (Figure 3A). At 142.20 s in the middle of the DCE droplet, a signal

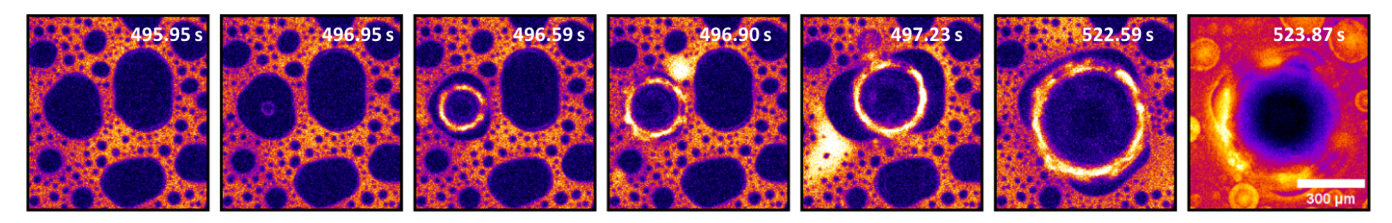


Figure 2. Nucleation and growth of  $CO_2$  gas bubble is marked by an expanding ring of light. At 495.95 s, the images show no bubble. The next image (496.95 s) shows the nucleation of the  $CO_2$  bubble marked by a small purple ring. At 496.59 s, the bubble grew, which is shown by a more intense and expanding ring of light. At 497.23 s, DCE droplet coalescence occurs and the ring of light ( $CO_2$  bubble) continues to grow. The image labeled with 522.59 s shows a much larger ring. Then, fluorescence was taken of the system while the ECL reaction was still running. The scale bar is 300  $\mu$ m.

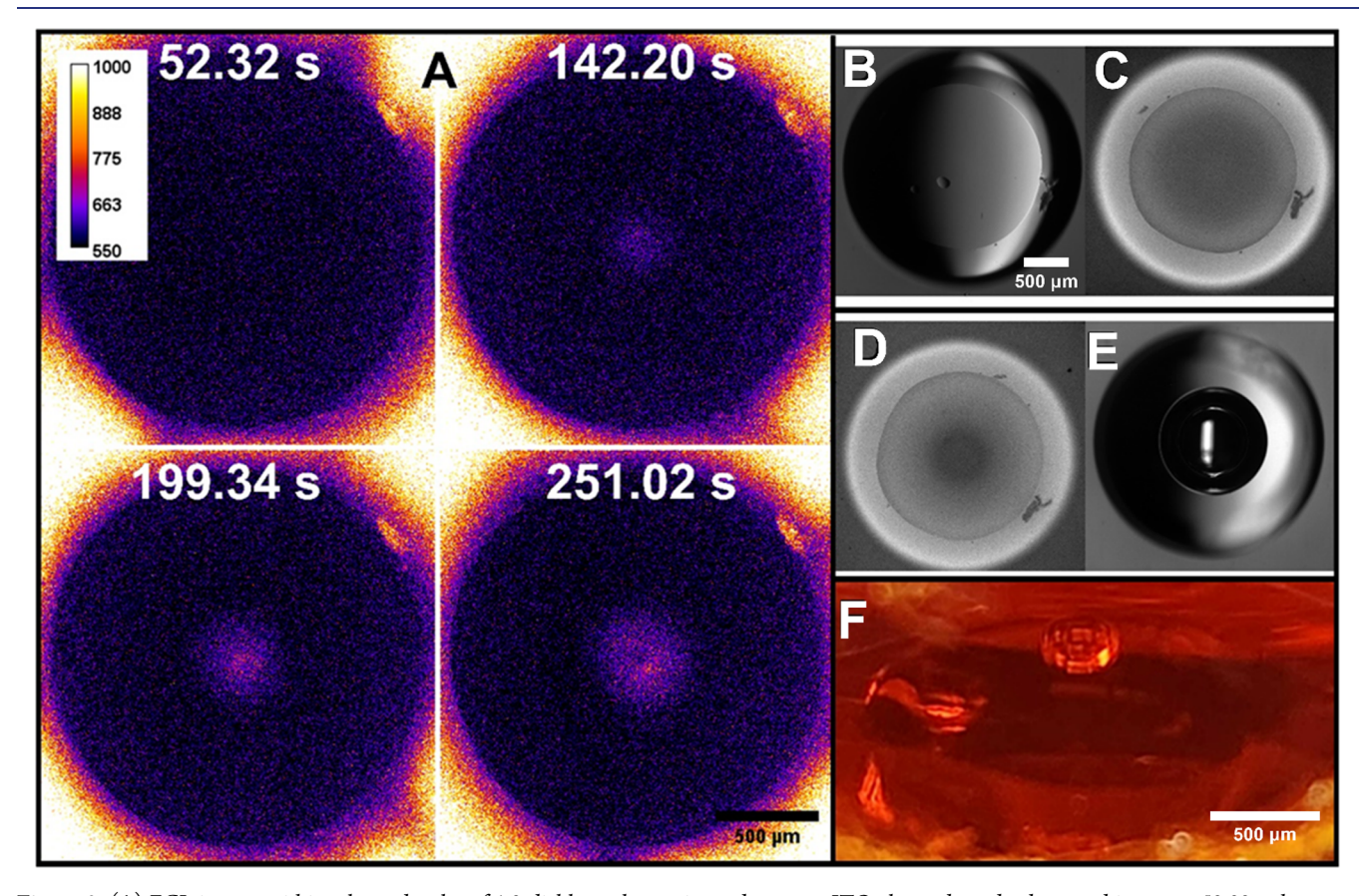


Figure 3. (A) ECL images within a large droplet of 1,2-dichloroethane pipetted onto an ITO electrode and submerged in water. 52.32 s shows no bubble reflection present. At 142.20 s, bubble nucleation starts. It then grows through the rest of the experiment. Images were taken with an EMCCD camera. (B) ITO focus level transmitted light bright-field before ECL. (C) Fluorescence at the ITO level before bubble formation and ECL. (D) Fluorescence at the ITO level after bubble nucleation. (E) Transmitted light bright-field at the bubble focus level. (B–E) Images taken with a CMOS camera. (F) Profile view of the pipetted DCE droplet and formed gas bubble. The image was acquired using a CMOS camera. To note, the  $CO_2$  bubble was continually growing after the ECL reaction was stopped. The profile view (F) was taken first, then the fluorescence (D), and then finally the transmitted light bright-field (E) with gaps of multiple minutes between them as cameras were changed and the height of the focal plane was adjusted. In panel E, the white streak in the black appearing  $CO_2$  bubble is the reflection from the light above. All the scale bars are 500  $\mu$ m.

appeared and grew in size and intensity through the rest of the 300 s experiment. Figure 3B,C shows transmitted light bright-field and fluorescence microscopy of the droplet, respectively, before the  $CO_2$  bubbles' appearance. To show the change in the system after ECL concluded, fluorescence at the level of the ITO electrode was imaged (Figure 3D). A dark, relatively diffuse circle can be observed, showing a decrease in the  $[Ru(bpy)_3]^{2+}$  fluorescence intensity. The objective was moved upward in the z direction to raise the focal plane to the height of the maximum circumference of the DCE droplet (Figure 3E). This shows a very symmetrical  $CO_2$  bubble with a

reflection of the transmitted light source as a white streak through the bubble. Additionally, shortly after the ECL reaction concluded, a profile view image of the DCE droplet was taken (Figure 3F).

Having now more critically established the geometry of the large  $\mathrm{CO}_2$  bubbles present in this confined multiphase system, we can construct a model. Figure 4 shows a schematic with the different pathways in which  $\mathrm{CO}_2$  bubbles can be trapped in the confined organic microenvironment.  $\mathrm{CO}_2$  molecules are produced by the decomposition of radical oxalate into  $\mathrm{CO}_2$  and  $\mathrm{CO}_2^{\bullet-}$ , with the later eventually being oxidized to produce

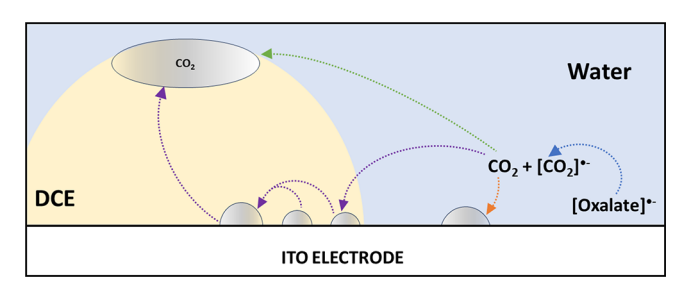
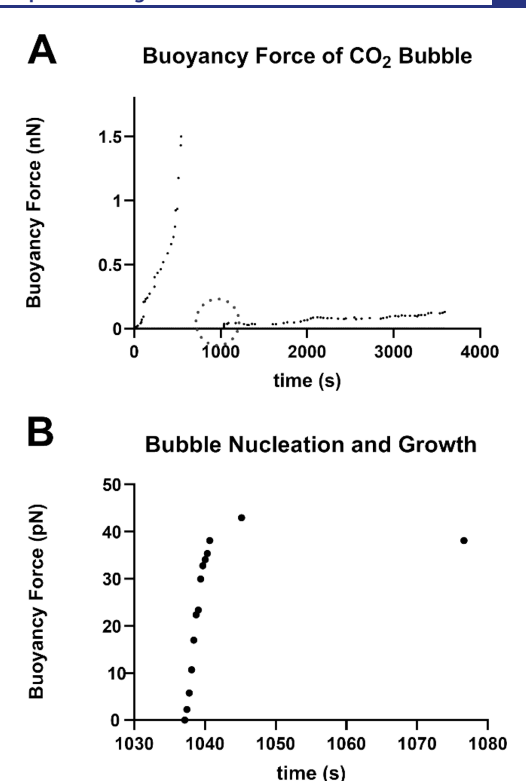


Figure 4. Scheme of the  $\mathrm{CO}_2$  bubble formation. The radical oxalate anion is produced through oxidation on the surface of the ITO electrode. This species then decomposes into carbon dioxide and its radical anion (blue arrow). This  $\mathrm{CO}_2$  has multiple pathways in which it can proceed. Following the orange arrow, the  $\mathrm{CO}_2$  can nucleate and then grow along the ITO surface in the aqueous phase. This bubble can then dislodge from the ITO electrode when the buoyancy force is great enough. The purple arrow shows the transport of the  $\mathrm{CO}_2$  molecules into the organic phase. Then, nucleation can occur along the surface of the ITO electrode. Also diagrammatically depicted is a dynamic physiochemical event such as bubble merging. These smaller bubbles will continue to grow, and when they gain a sufficient size, they can detach, due to the buoyancy force, and merge with the larger bubble above. Meanwhile, in following the green arrow, the  $\mathrm{CO}_2$  molecules can join the large bubble trapped at the interface.

another CO<sub>2</sub> molecule (Figure 1). Specifically, there are a few different pathways for the CO2 molecule to go. First, there can be a nucleation event at the electrode surface in the aqueous phase (orange arrow). This bubble on the ITO surface can detach due to the buoyancy force exerted and be transported into the atmosphere above the electrochemical cell. This would be the same pathway for CO<sub>2</sub> bubbles if there was no 1,2dichloroethane present (Figure S2). Conversely, when DCE droplets are present on the surface of the ITO electrode, the CO<sub>2</sub> molecules can be transported into the organic phase and nucleate bubbles along the electrode surface (Figure 4, purple arrows, and Figure S3). These bubbles can undergo physiochemical events like merging. When the force of buoyancy is great enough to overcome the surface tension at the electrodelelectrolyte interface, the CO2 bubble will leave and be trapped at the apex of the organiclaqueous interface, as shown on a single droplet in Figure 3. We can observe bubble growth at both the electrodelelectrolyte and water11,2dichloroethane interfaces (Figure S3).

Finally, once the apex of the organic—aqueous interface has a CO<sub>2</sub> bubble present, it can act as a reservoir for dissolved CO<sub>2</sub> molecules (Figure 4, green arrow). Throughout the experiments, the CO<sub>2</sub> bubble trapped at the waterl1,2-dichloroethane interface continuously grows, most likely pointing to a combination of pathways. When the force of buoyancy becomes greater than the surface tension present at the waterl1,2-dichloroethane interface, the bubble will leave, often causing a reorganization event for the DCE droplet (Figure S4).

Using ImageJ, the lifetime diameters of  $CO_2$  bubbles were tracked for a selected 1,2-dichloroethane droplet over an hourlong experiment (Figure 5A,B). This through-space ECL signal allows us to approximate the buoyancy force acting upon the bubble by measuring the diameter of the ring of light. Full assumptions and equations for calculating the bubble buoyancy force are given below. The force of buoyancy ( $F_B$ ) for an object can be calculated by multiplying the density of fluid ( $\rho$ ), the displaced volume (V), and the acceleration due to gravity (9.81 m•s<sup>-2</sup>).



**Figure 5.** (A) Assuming a spherical shape, the buoyancy force of the  $\mathrm{CO}_2$  bubble in the selected droplet during the hour-long experiment was calculated at the organiclaqueous interface. The internal diameter of the light ring was measured using ImageJ. Seen between 0 and 1000 s is the nucleation, growth, and eventual expulsion of the first  $\mathrm{CO}_2$  bubble. After 1000 s is the nucleation and growth of the second  $\mathrm{CO}_2$  bubble in the same DCE droplet. (B) The second graph shows a closer view over 50 s of this nucleation and growth of the  $\mathrm{CO}_2$  bubble.

$$F_{\rm R} = \rho V g \tag{1}$$

At the interface, assuming that the total volume displaced in the 1,2-dichlorethane ( $V_{\rm DCE}$ ) and water ( $V_{\rm water}$ ) phase is equal, and assuming a sphere shape for the CO<sub>2</sub> bubble, the two displaced volume elements, by phase, can be represented as  $V_i$  for 1/2 of a sphere.

$$V_{\text{total}} = V_{\text{water}} + V_{\text{DCE}} \tag{2}$$

$$V_{\text{water}} = V_{\text{DCE}}$$
 (3)

$$\frac{1}{2}V_{\text{total}} = V_i \tag{4}$$

$$V_{i} = \frac{1}{2} \left( \frac{4}{3} \pi \left( \frac{d}{2} \right)^{3} \right) = \frac{\pi}{12} d^{3}$$
 (5)

Given that the CO<sub>2</sub> bubble is at an interface, there will be two separate density components between the two phases that can be represented with eq 6. The densities of  $\rho_{\text{water}}$  and  $\rho_{\text{DCE}}$  are 0.997 and 1.245 g•cm<sup>3</sup>, respectively.<sup>25,26</sup>

$$\rho_{\text{system}} = \rho_{\text{water}} + \rho_{\text{DCE}} \tag{6}$$

By combining eqs 1, 5, and 6, with the given assumptions, we can form eq 7.

$$F_{\rm B} = \frac{\pi g}{12} d^3 (\rho_{\rm water} + \rho_{\rm DCE}) \tag{7}$$

Equation 7 reveals a direct connection between the buoyancy force of a  $CO_2$  bubble at an interface  $(F_B)$  with the measured diameter (d) of the bubble through through-space ECL.

From 0 to 544 s, a CO<sub>2</sub> bubble grows until it gets ejected from the 1,2-dichloroethane droplet and reorganizes at the electrode surface (Figure S6). At 1037 s, droplet nucleation occurs quickly, followed by rapid growth through 1041 s. After the rapid growth, slow growth continues through the rest of the experiment. This shows an important characteristic of this system in which the 1,2-dichloroethane droplets can have multiple bubble nucleation throughout the lifetime. While not examined in Figure 4, 1,2-dichloroethane droplets with CO<sub>2</sub> bubbles can also coalesce and exhibit bubble coalescence as well (Figure S5). Like the reorganization, there tends to be a large increase in the ECL signal after the DCE droplets coalesce, allowing for a fresh ITO surface to be exposed; thus, mass transport of the coreactant and luminophore occurs more readily following the convection currents of the moving interface.

#### CONCLUSIONS

In this article, we have demonstrated that ECL can be used to examine entities, such as CO<sub>2</sub> bubbles, that are located far away (remotely) from the electrode surface. While it has been established that ECL emission occurs only within a few micrometers of the electrode surface, the light path can be altered by reflection and/or refraction off phase boundaries (such as the gaslliquid interface). We have termed this signal "through-space ECL" since it is fundamentally different from the emission at the electrode surface due to the intermediate reflection step. Through-space ECL offers a change to the status quo paradigm of ECL since three-dimensional geometric information about an environment can now be extracted from a pseudo-two-dimensional process. To examine this phenomenon, we used oxalate that decomposes to two CO<sub>2</sub> molecules via a strong reducing agent. Since CO<sub>2</sub> is much more soluble in the organic phase (1,2-dichloroethane) than in the aqueous phase, the organic droplets act as a reservoir for the CO<sub>2</sub>. This leads to bubble nucleation and growth initially at the electrodel electrolyte interface, where bubbles coalesce, and then to bubble entrapment at the water1,2-dichloroethane interface. Our analyses reveal the buoyancy force exerted on the bubble trapped at the liquidliquid phase boundary.

Recently, phase boundary reactivity has been implicated in driving curious chemistry, such as the generation of unfavorable species  $^{27-30}$  and reaction acceleration.  $^{11,31,32}$ New measurement tools are necessary to elucidate such fundamental tenets of nature. Our presented technique was designed to probe such phase boundaries, and we have come across the rather interesting observation, and the topic of the current article, that microbubbles generated in the microenvironment get trapped at liquidlliquid phase boundaries far away from the electrode. We also show that this is a general phenomenon (see Supporting Information Figure S7). The same technique could also be used for other through-space ECL studies, such as imaging single cells, 33 phase boundaries within cells, and bead-based assays.<sup>34</sup> The presented technique yields unique information regarding interfacial chemistry and offers new spectroelectrochemical tools to study the curious chemistry of phase boundary reactivity.

#### MATERIALS AND METHODS

Tetrabutylammonium perchlorate (99%), 1,2-dichloroethane (99.8%), and sodium oxalate (99%) were purchased from Sigma-Aldrich. Tris(bipyridine)ruthenium(II) chloride hexahydrate ([Ru-(bpy)\_3][Cl\_2] $\bullet$ 6H<sub>2</sub>O, 98%) was purchased from Acros Organics and was kept under argon. All chemicals were used without further purification steps, unless noted otherwise.

The emulsion was prepared based on and adapted from a previously published methodology.  $^{16}$  In a 20 mL scintillation vial, an aliquot containing 300  $\mu\text{L}$  of dichloroethane containing 100 mM tetrabutylammonium perchlorate (TBAP) was added to 5 mL of ultrapure water (>18.20 M $\Omega$ ·cm, Thermo Scientific) containing 10 mM tris(bipyridine)ruthenium(II) chloride hexahydrate and 50 mM sodium oxalate. The solution was ultrasonicated (500 W, 40% amplitude) on a pulsing method constructed by 5 on 5 s off for 10 total cycles.

The microscope and imaging system were composed of a Leica DMi8 microscope (Leica Microsystems, Germany) equipped with a pE-300lite light source (CoolLED, United Kingdom). Fluorescence was taken with the Y3 filter (Leica Microsystems, Germany) that has an excitation of 532–558 nm, a dichroic mirror at 565 nm, and an emission of 570–640 nm. The objective used was 5× with a numerical aperture of 0.12. Two cameras were used: a complementary metal-oxide semiconductor camera (Orca-Quest qC-MOS C15550-20UP from Hamamatsu, Hamamatsu, Japan) and an EMCCD iXon 897 camera (Andor Technology Ltd., Belfast, UK) set at a 100 ms exposure time, a 10 MHz quality mode, a 4.22  $\mu$ s shift speed, and a temperature of -75 °C, resulting in a frame rate of 0.321 s. All images were analyzed using ImageJ. All optical acquisitions were conducted through the LAS X software (Leica Microsystems, Germany).

A CHI 920D scanning electrochemical microscope (CH Instruments, Austin, TX) was used to perform the electrochemical experiments. The reference electrode (CH Instruments, Austin, TX) was composed of an Ag/AgCl (1 M KCl) electrode and a salt bridge composed of agarose and 1 M KCl in a glass pipet to protect the reference electrode from exposure to nonaqueous solvents like DCE. The ITO working electrode (Huany Co., China) was cut into square pieces approximately 25 mm  $\times$  25 mm. The resulting ITO pieces were epoxied onto circular glass tubes with an approximate radius of 19 mm and a height of 20 mm. A glassy carbon rod (r = 1.5 mm, L = 10 cm, CH Instruments, Austin, TX) was used as the counter electrode and was submerged approximately 1.5 cm into solution. The emulsion was then decanted into the cell.

#### ASSOCIATED CONTENT

#### **Solution** Supporting Information

The Supporting Information is available free of charge at https://pubs.acs.org/doi/10.1021/jacs.3c10505.

Chronoamperogram and optical and ECL images of bubble formation in multiphase environments (PDF)

#### AUTHOR INFORMATION

#### **Corresponding Author**

Jeffrey E. Dick — Department of Chemistry and Elmore Family School of Electrical and Computer Engineering, Purdue University, West Lafayette, Indiana 47907, United States; orcid.org/0000-0002-4538-9705; Email: jdick@purdue.edu

#### **Author**

Brady R. Layman – Department of Chemistry, Purdue University, West Lafayette, Indiana 47907, United States; orcid.org/0000-0002-8077-8490

Complete contact information is available at: https://pubs.acs.org/10.1021/jacs.3c10505

#### **Notes**

The authors declare no competing financial interest.

#### ACKNOWLEDGMENTS

We acknowledge financial support from the Chemical Measurement and Imaging Program in the National Science Foundation Division of Chemistry under grant CHE-2003587/2319925. We thank Dr. Christophe Renault (Layola University Chicago), Kathryn J. Vannoy (Purdue University), and Thomas B. Clarke (Purdue University) for insightful discussions. Additionally, we would like to thank Patrick J. Herchenbach for experimental support that went toward Figure S7. The TOC graphic was created with the use of the artificial intelligence platform OpenAI.

#### REFERENCES

- (1) Colón-Quintana, G. S.; Clarke, T. B.; Dick, J. E. Interfacial solute flux promotes emulsification at the waterloil interface. *Nat. Commun.* **2023**, *14*, 705.
- (2) Colón-Quintana, G. S.; Vannoy, K. J.; Renault, C.; Voci, S.; Dick, J. E. Tuning the Three-Phase Microenvironment Geometry Promotes Phase Formation. *J. Phys. Chem. C* **2022**, *126* (47), 20004–20010.
- (3) Zwicker, D.; Seyboldt, R.; Weber, C. A.; Hyman, A. A.; Jülicher, F. Growth and division of active droplets provides a model for protocells. *Nature Physics.* **2017**, *13* (4), 408–413.
- (4) Brangwynne, C. P.; Eckmann, C. R.; Courson, D. S.; Rybarska, A.; Hoege, C.; Gharakhani, J.; Jülicher, F.; Hyman, A. A. Germline P granules are liquid droplets that localize by controlled dissolution/condensation. *Science* **2009**, *324* (5935), 1729–1732.
- (5) Voci, S.; Clarke, T. B.; Dick, J. E. Abiotic Microcompartments Form When Neighbouring Droplets Fuse: an Electrochemiluminescence Investigation. *Chem. Sci.* **2023**, *14*, 2336–2341.
- (6) Song, X.; Meng, Y.; Zare, R. N. Spraying Water Microdroplets Containing 1,2,3-Triazole Converts Carbon Dioxide into Formic Acid. J. Am. Chem. Soc. 2022, 144 (37), 6744–16748.
- (7) Song, X.; Basheer, C.; Zare, R. N. Making ammonia from nitrogen and water microdroplets. *Proc. Natl. Acad. Sci. U. S. A.* **2023**, 120, No. e2301206120.
- (8) Lee, J. K.; Samanta, D.; Nam, H. G.; Zare, R. N. Micrometer-Sized Water Droplets Induce Spontaneous Reduction. *J. Am. Chem. Soc.* **2019**, *141* (27), 10585–10589.
- (9) Lee, J. K.; Samanta, D.; Nam, H. G.; Zare, R. N. Spontaneous Formation of Gold Nanostructures in Aqueous Microdroplets. *Nat. Commun.* **2018**, *9*, 1562.
- (10) Holden, D. T.; Morato, N. M.; Cooks, R. G. Aqueous microdroplets enable abiotic synthesis and chain extension of unique peptide isomers from free amino acids. *Proc. Natl. Acad. Sci. U.S.A.* **2022**, *119* (42), No. e2212642119.
- (11) Vannoy, K. J.; Lee, I.; Sode, K.; Dick, J. E. Electrochemical Quantification of Accelerated FADGDH Rates in Aqueous Nanodroplets. *Proc. Natl. Acad. Sci. U. S. A.* **2021**, *118* (25), No. e2025726118.
- (12) Sojic, N. Analytical Electrogenerated Chemiluminescence: From Fundamentals to Bioassays. Royal Society of Chemistry, 2019 DOI: 10.1039/9781788015776.
- (13) Voci, S.; Goudeau, B.; Valenti, G.; Lesch, A.; Jovic, M.; Rapino, S.; Paolucci, F.; Arbault, S.; Sojic, N. Surface-Confined Electrochemiluminescence Microscopy of Cell Membranes. *J. Am. Chem. Soc.* **2018**, *140*, 14753–14760.
- (14) Hu, L.; Xu, G. Applications and Trends in Electrochemiluminescence. Chem. Soc. Rev. 2010, 39, 3275–3304.
- (15) Bois, R.; Scarabino, S.; Ravaine, V.; Sojic, N. Two-Dimensional Electrochemiluminescence: Light Emission Confined at the Oil—Water Interface in Emulsions Stabilized by Luminophore-Grafted Microgels. *Langmuir.* **2017**, *33*, 7231–7238.

- (16) Glasscott, M. W.; Dick, J. E. Visualizing Phase Boundaries with Electrogenerated Chemiluminescence. *J. Phys. Chem. Lett.* **2020**, *11* (12), 4803–4808.
- (17) Bard, A. J. Electrogenerated Chemiluminescence; CRC Press, 2019 DOI: 10.1201/9780203027011.
- (18) Dick, J. E.; Renault, C.; Kim, B. K.; Bard, A. J. Electrogenerated Chemiluminescence of Common Organic Luminophores in Water Using an Emulsion System. *J. Am. Chem. Soc.* **2014**, *136*, 13546–13549.
- (19) Layman, B. R.; Dick, J. E. Phase-Resolved Electrochemiluminescence with a Single Luminophore. *J. Phys. Chem. Lett.* **2023**, *14* (36), 8151–8156.
- (20) Rubinstein, I.; Bard, A. J. Electrogenerated Chemiluminescence. 37. Aqueous Ecl Systems Based on Tris(2,2'-Bipyridine)Ruthenium-(2+) and Oxalate or Organic Acids. *J. Am. Chem. Soc.* **1981**, *103*, 512–516.
- (21) Pachauri, R. K.; Allen, M.; Barros, V.; Broome, J.; Cramer, W.; Christ, R.; Church, J.; Clarke, L.; Dahe, Q.; Dasgupta, P.; Dubash, N. K.; Edenhofer, O.; Elgizouli, I.; Field, C. B.; Forster, P.; Fuglestvedt, J.; Gomez-Echeverri, L.; Hallegatte, S.; Hegerl, G.; Howden, M.; Jiang, K.; Jimenez Cisneroz, B.; Kattsov, V.; Lee, H.; Mach, K. J.; Marotzke, J.; Mastrandrea, M. D.; Meyer, L.; Minx, J.; Mulugetta, Y.; O'Brien, K.; Oppenheimer, M.; Pereira, J. J.; Pichs-Madruga, R.; Plattner, G. K.; Pörtner, H. O.; Power, S. B.; Preston, B.; Ravindranath, N. H.; Reisinger, A.; Riahi, K.; Rusticucci, M.; Scholes, R.; Seyboth, K.; Sokona, Y.; Stavins, R.; Stocker, T. F.; Tschakert, P.; van Vuuren, D.; van Ypserle, J. P. Climate Change 2014: Synthesis Report. Contribution of Working Groups I, II and III to the Fifth Assessment Report of the Intergovernmental Panel on Climate Change. Intergovernmental Panel on Climate Change. Geneva, Switzerland, 2014.
- (22) Novek, E. J.; Shaulsky, E.; Fishman, Z. S.; Pfefferle, L. D.; Elimelech, M. Low-Temperature Carbon Capture Using Aqueous Ammonia and Organic Solvents. *Environ. Sci. Technol. Lett.* **2016**, 3 (8), 291–296.
- (23) Peng, S.; Mega, T. L.; Zhang, X. Collective Effects in Microbubble Growth by Solvent Exchange. *Langmuir.* **2016**, 32 (43), 11265–11272.
- (24) Peng, S.; Spandan, V.; Verzicco, R.; Lohse, D.; Zhang, X. Growth dynamics of microbubbles on microcavity arrays by solvent exchange: Experiments and numerical simulations. *J. Colloid Interface Sci.* **2018**, 532, 103–111.
- (25) Wagner, W.; Pruss, A. The IAPWS Formulation 1995 for the Thermodynamic Properties of Ordinary Water Substance for General and Scientific Use. J. Phys. Chem. Ref. Data 2002, 31 (2), 387–535.
- (26) Haynes, W. M. (ed.). CRC Handbook of Chemistry and Physics. CRC Press LLC, 2015 DOI: 10.1201/b17118.
- (27) Mehrgardi, M. A.; Mofidfar, M.; Zare, R. N. Sprayed Water Microdroplets Are Able to Generate Hydrogen Peroxide Spontaneously. *J. Am. Chem. Soc.* **2022**, *144* (17), 7606–7609.
- (28) Vogel, Y. B.; Evans, C. W.; Belotti, M.; Xu, L.; Russell, I. C.; Yu, L.; Fung, A. K. K.; Hill, N. S.; Darwish, N.; Gonçales, V. R.; Coote, M. L.; Iyer, K. S.; Ciampi, S. The Corona of a Surface Bubble Promotes Electrochemical Reactions. *Nat. Commun.* 2020, *11*, 6323.
- (29) Gallo, A., Jr; Musskopf, N. H.; Liu, X.; Yang, Z.; Petry, J.; Zhang, P.; Thoroddsen, S.; Im, H.; Mishra, H. On the Formation of Hydrogen Peroxide in Water Microdroplets. *Chem. Sci.* **2022**, *13*, 2574–2583.
- (30) Ben-Amotz, D. Electric Buzz in a Glass of Pure Water. Science 2022, 376, 800-801.
- (31) Wei, Z.; Li, Y.; Cooks, R. G.; Yan, X. Accelerated Reaction Kinetics in Microdroplets: Overview and Recent Developments. *Annu. Rev. Phys. Chem.* **2020**, *71*, 31–51.
- (32) Li, Y.; Liu, Y.; Gao, H.; Helmy, R.; Wuelfing, W. P.; Welch, C. J.; Cooks, R. G. Accelerated Forced Degradation of Pharmaceuticals in Levitated Microdroplet Reactors. *Chem.—Eur. J.* **2018**, *24* (29), 7349–7353.
- (33) Valenti, G.; Scarabino, S.; Goudeau, B.; Lesch, A.; Jović, M.; Villani, E.; Sentic, M.; Rapino, S.; Arbault, S.; Paolucci, F.; Sojic, N.

Single Cell Electrochemiluminescence Imaging: From the Proof-of-Concept to Disposable Device-Based Analysis. *J. Am. Chem. Soc.* **2017**, *139*, 16830–16837.

(34) Han, D.; Fang, D.; Valenti, G.; Paolucci, F.; Kanoufi, F.; Jiang, D.; Sojic, N. Dynamic Mapping of Electrochemiluminescence Reactivity in Space: Application to Bead-Based Assays. *Anal. Chem.* **2023**, 95 (42), 15700–15706.

### **□** Recommended by ACS

## Exploitation of Luminescent Lanthanide Nanoparticles for a Sensitivity-Enhanced ELISA Detection Method

Ali A. Kassir, Loïc J. Charbonnière, et al.

JANUARY 26, 2024

ANALYTICAL CHEMISTRY

READ 🗹

## Imaging Single $H_2$ Nanobubbles Using Off-Axis Dark-Field Microscopy

Milomir Suvira, Bo Zhang, et al.

OCTOBER 18, 2023

ANALYTICAL CHEMISTRY

READ 🗹

### **Development of an Electrochemical, Aptamer-Based Sensor** for Dynamic Detection of Neuropeptide Y

Jordan M. Seibold, Ryan J. White, et al.

NOVEMBER 30, 2023

ACS SENSORS

READ 🗹

#### Impact of Surface Chemistry on Emulsion-Electrode Interactions and Electron-Transfer Kinetics in the Single-Entity Electrochemistry

Minshu Du, Feng Liu, et al.

JANUARY 05, 2024

ANALYTICAL CHEMISTRY

READ 🗹

Get More Suggestions >